THE AMERICAN SOCIETY OF MECHANICAL ENGINEERS
345 E. 47th St., New York, N.Y. 10017

98-GT-402

ENTRANCE EFFECTS ON DIFFUSED FILM-COOLING HOLES

A. Kohli* and K. A. Thole
Mechanical Engineering Department
University of Wisconsin
Madison, Wisconsin 53706

Abstract

Film-cooling is a widely used method of prolonging blade life in high performance gas turbines and is implemented by injecting cold air through discrete holes on the blade surface. Most experimental research on film-cooling has been performed using round holes supplied by a stagnant plenum. This can be quite different from the actual turbine blade conditions in that a crossflow may be present whereby the internal channel Reynolds number could be as high as 90,000. This computational study uses a film-cooling hole that is inclined at 35° with respect to the mainstream and is diffused at the hole exit by 15°. An engine representative jet-to-mainstream density ratio of two was simulated. The test matrix consisted of fourteen different cases that were simulated for the two different blowing ratios in which the following effects were investigated: a) the effect of the orientation of the coolant supply channel relative to the cooling hole, b) the effect of the channel Reynolds number, and c) the effect of the metering length of the cooling hole. Results showed that the orientation of the coolant supply had a large effect whereby the worst orientation, in terms of a reduced adiabatic effectiveness, was predicted when the channel supplying the cooling hole was perpendicular to the mainstream. For this particular orientation, higher laterally averaged effectiveness occurred at lower channel Reynolds numbers and with the hole having a short metering length.

Introduction

Making the most effective use of the coolant fluid for a turbine blade, which is bleed air extracted from the turbine working fluid, is the aim for many turbine designers. This coolant fluid is used to convectively cool the inside of the blade through passages as well as inside discrete cooling holes placed in the blade surface. After exiting from the holes, the fluid provides film-cooling on the outside blade surface. Over the years, experimental and computational studies have identified key scaling parameters for film-cooling flows, such as momentum flux for a round hole, that dictate the performance of those flows. There have been relatively few studies, however, that have evaluated the effects that the entrance crossflow conditions have on the exiting coolant flow, which is not fully developed since it typically exits from holes that are quite short.

The overall goal of this CFD study was to perform a systematic investigation on the effects of entrance crossflow conditions on adiabatic effectiveness for a film-cooling hole geometry that has an inclination angle of 35° and is fully expanded by 15°. Specifically, this study investigated the effects of: 1) supply channel crossflow orientation, 2) blowing ratio, 3) supply channel Reynolds number, and 4) metering length of the film-cooling hole. To investigate the effect of supply channel orientation, crossflow that was co-flowing ($\phi = 0°$), counter-flowing ($\phi = 180°$), and perpendicular ($\phi = 90°$) to that of the mainstream direction were considered in this study. These results were compared to those obtained for a stagnant plenum as has been the case in most film-cooling literature. By comparing results for two blowing ratios, $M = 1$ and 2, the effects for different crossflow conditions was investigated. In order to study the effect of supply channel Reynolds number it was varied between $10{,}000 < Re < 90{,}000$ for a fixed blowing ratio and crossflow orientation. Another parameter which greatly influences the flow through an expanded hole is the cylindrical portion (metering length) upstream of the expansion. To study this effect the metering length of the cooling hole was varied between, $1 < L_M/D < 4$ for two different crossflow orientations.

The following sections discuss past relevant studies, the CFD method used in this study and some benchmark results, present results for the shaped cooling hole, and finally give some conclusions.

Relevant Past Studies

Although the literature indicates that there is a large effect of the coolant supply channel on adiabatic effectiveness, as illustrated by the recent measurements presented by Gritsch, et al. (1997a), there have been only a few studies that have investigated the effect of the supply channel crossflow. The 15° fully expanded cooling hole measurements, reported by Gritsch, et al. (1997a) showed that for blowing ratios of $M = 1$ and 1.5 reduced values of laterally averaged adiabatic effectivenesses occurred when the supply channel crossflow was turned perpendicular (ϕ

* Present address is Pratt & Whitney, 400 Main Street, MS 169-02, East Hartford, CT 06108

Presented at the International Gas Turbine & Aeroengine Congress & Exhibition
Stockholm, Sweden — June 2–June 5, 1998

= 90°) as compared to the case when there was a co-flowing supply (ϕ = 0°). For the same mainstream and coolant supply channel conditions, their results for the round hole indicated no effect at a near-optimal blowing ratio of M = 0.5. At a higher mass flux ratio of M = 1, complementary flowfield studies reported by Thole, et al. (1997) indicated there were significant flowfield differences as the channel Reynolds number increased for a co-flowing channel. The adiabatic effectiveness levels for the round hole had the opposite trend to the shaped hole in that at higher blowing ratios for the round hole higher values of laterally averaged effectiveness occurred for the ϕ = 90° supply flow direction as compared to the ϕ = 0° supply flow direction. Since the jet is known to separate at a blowing ratio of M = 1 for a round hole (Sinha, et al., 1991), this opposite trend may be occurring due to the swirling of the jet inside the hole, which will be discussed later in this paper, thereby causing a reduction in the severity of the jet detachment.

Hay, et al. (1983) showed that the crossflow at the jet entrance had a large effect on the discharge coefficient relative to the effect of the crossflow at the hole exit. For example, in the case where there was a co-flowing channel at the hole entrance, as the velocity in the channel increased from $Ma_c = 0$ to $Ma_c = 0.4$ the discharge coefficient increased by 30%. In contrast, as the exit Mach flow increased from $Ma_\infty = 0$ to $Ma_\infty = 0.5$, the discharge coefficient decreased by only 10% for pressure ratios of $1.05 < P_c/p_\infty < 1.4$ and remained constant when the pressure ratios were $P_c/p_\infty > 1.4$. Similar results were obtained in a recent study involving holes with expanded exits by Gritsch, et al. (1997b). They reported an increase in the discharge coefficient of 40% when the crossflow at the hole entrance was increased from $Ma_c = 0$ to $Ma_c = 0.6$.

In their CFD study, Berhe and Patankar (1996) investigated the effect of supplying the coolant to a plenum from different directions, which is distinctly different than investigating the effect of supplying the cooling hole from different channel flow directions, where there is an inlet and an exit to the channel. The results of Berhe and Patankar showed that at a blowing ratio of M = 0.5 and a plenum height of 1D, the adiabatic effectiveness was reduced when the coolant was introduced into the plenum flowing in the parallel but opposite direction (counter-flowing) as the flow at the hole exit.

Burd and Simon (1997) used the same strategy as Berhe and Patankar (1996) whereby they supplied the plenum for their coolant hole from different directions and the only flow exiting the plenum was through the cooling hole. Similar to the results reported by Gritsch, et al. (1997a) for a round film-cooling hole, Burd and Simon (1997) showed that at a low mass flux ratio of M = 0.5 there was no effect of the orientation of their plenum supply on the laterally averaged effectiveness values. At a high mass flux ratio of M = 1, however, Burd and Simon found that the laterally averaged effectiveness values were higher for the counter-flow supply to the plenum. Because this high mass flux ratio jet is also at a high momentum flux ratio (I = 1), the jet is separated from the downstream surface. The counter-flow plenum actually helps improve the laterally averaged effectiveness for the separated jet condition since it increases the separation region inside the cooling hole on the leeward side causing very high velocity coolant to exit from the upstream side of the cooling hole. Burd and Simon (1997) attributed this improvement to the fact that because the coolant is exiting from the upstream side of the hole, there is enough streamwise distance to allow the jet to be pushed down before encountering the downstream surface.

Kohli and Thole (1997) presented results from a CFD study in which they compared the performance of a round film-cooling hole to that of a diffused film cooling hole with the same geometry used for the study presented in this paper (15° expanded cooling hole). With a fixed channel Reynolds number, they determined the effect that different crossflow directions at the hole entrance had on adiabatic effectiveness values. They showed that the shaped cooling hole was significantly affected by the flow direction of the coolant supply channel in that 'hot mainstream' ingestion into the cooling hole was the highest for the ϕ = 90° case. The hot mainstream ingestion was a key effect in reducing the lateral averaged effectiveness whereby this ingestion was caused by a vortex entraining mainstream fluid into the cooling hole. The ingestion for both the plenum and ϕ = 180° cases, were similar and somewhat less while for the ϕ = 0° case the least amount of ingestion occured.

It is clear from the literature that currently there are only a few effects that have been studied with regards to the entrance conditions of film-cooling holes. This paper presents results from fourteen different cases whereby the effects of metering hole length, supply channel direction, and supply channel Reynolds number have been studied at two mass flux ratios.

Computational Domain and Code Description

The diffused cooling hole geometry, which will be discussed in further detail in the following section is shown in Figure 1 while the computational domain, which consists of the mainstream flow, the diffused film-cooling hole, and the supply channel, is shown in Figure 2. The streamwise extent of the computational domain, similar to the past CFD study by Berhe and Patankar(1996), was $-19 \le x/D \le 30$. A uniform inlet

Nomenclature

C_D	=	discharge coefficient
DR	=	density ratio, $DR = \rho_j/\rho_\infty$
H	=	height of supply channel
I	=	momentum flux ratio, $I = \rho_j V_j^2 / \rho_\infty U_\infty^2$
k	=	turbulent kinetic energy, $k = 3/2\,(U_\infty Tu(\%)/100)^2$
L	=	length of film cooling hole
L_M	=	cylindrical metering length
M	=	blowing ratio, $M = \rho_j V_j/\rho_\infty U_\infty$
Ma	=	Mach number
p	=	static pressure
P	=	pitch distance between film cooling holes
P_c	=	total pressure in coolant channel
Re	=	Reynolds number using inlet velocity and channel height
Tu	=	turbulence level, $Tu = 100\,(2/3\,k)^{0.5}/U_\infty$
V	=	velocity magnitude
x	=	streamwise direction, see Figure 1
y	=	vertical direction, see Figure 1
z	=	spanwise direction from hole center

Greek

α	=	injection angle of film cooling holes
ε	=	turbulent dissipation rate, $\varepsilon = C_\mu^{3/4} k^{3/2} / D$
ρ	=	density
ϕ	=	angle between supply channel flow and mainstream
η	=	adiabatic effectiveness, $\eta = (T_{aw} - T_\infty) / (T_j - T_\infty)$
θ	=	momentum thickness
Θ	=	normalized temperature, $\Theta = (T - T_\infty) / (T_j - T_\infty)$
$\bar{\bar{\Theta}}$	=	spatially averaged jet temperatures inside the cooling hole

Subscripts

aw	=	adiabatic wall
c	=	coolant
Cl	=	centerline
∞	=	freestream
j	=	jet

Superscripts

$\bar{}$	=	laterally averaged
$\bar{\bar{}}$	=	area averaged

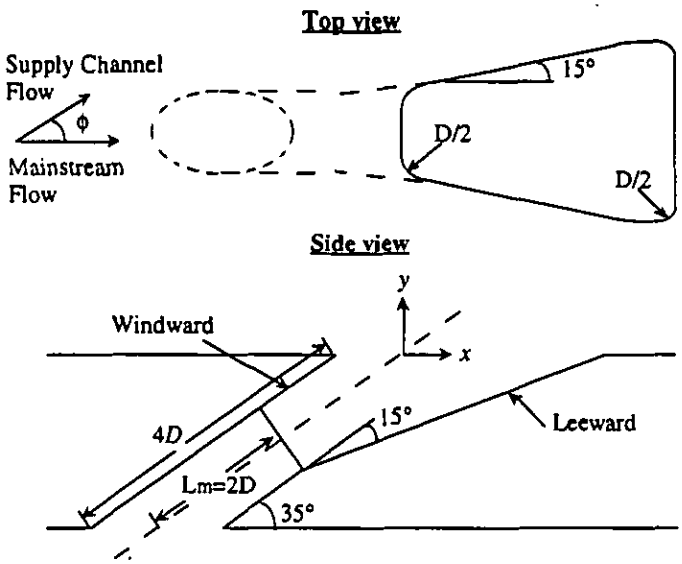

Fig. 1.Schematic of the shaped film-cooling hole geometry.

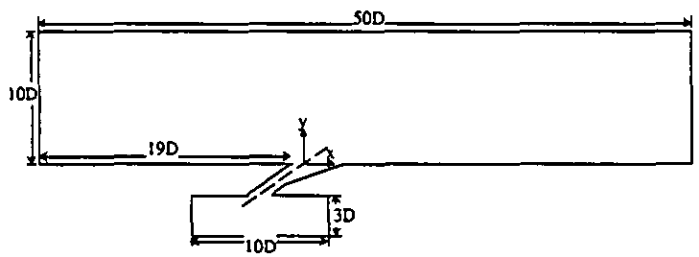

Fig. 2. Schematic of the computational domain used in this study, showing the extent of the mainstream flow, supply channel and film-cooling hole.

velocity is applied as a boundary condition at the upstream end of the domain. For the present study, with a freestream velocity of U_∞ = 10 m/s, this resulted in a Reynolds number of Re_θ = 560 upstream of the film-cooling holes. An outflow boundary condition is applied at the downstream end of the domain since the gradients in the streamwise direction are expected to be small at x/D = 30. In the vertical direction, the computational domain extends out to y/D = 10 which is sufficiently far away from the film-cooling flowfield to impose a zero gradient boundary condition.

For the case where the coolant supply channel is a plenum and for the case when flow in the supply channel is co-flowing ($\phi = 0°$) or counter-flowing ($\phi = 180°$) to that of the mainstream flow, a symmetry condition is applied on both the jet centerline and the half-pitch line. Therefore, for these cases the spanwise extent of the computational domain is only $-3 < z/D < 0$ and flow in only half the film-cooling hole is modeled. When the flow in the supply channel is in a direction perpendicular ($\phi = 90°$) to that of the mainstream flow, this symmetry condition cannot be applied at the jet centerline. In this case, the entire film cooling hole is modeled and the domain extends from $-3 < z/D < 3$ with periodic boundary conditions applied at both half-pitch lines.

The supply channel had a height of H/D = 3 and extends 5D upstream and 5D downstream of the entrance to the film-cooling hole. A uniform inlet velocity was imposed at the upstream end of the supply channel while the velocity at the outlet of the supply channel was set according to the desired blowing ratio. Mass conservation was checked to insure that the correct blowing ratio was maintained through the cooling hole and was within 0.1% of the desired value. For a channel inlet velocity of 3.5 m/s the boundary layer developing along the supply channel walls was 4 mm thick (0.3D) at a location one diameter upstream of the hole entrance. For the supply channel flow in a direction normal to the mainstream flow, the supply channel was rotated about its vertical axis by 90° and flow was considered to be in the -z direction. For the plenum case, the same supply channel geometry was used with an appropriate inlet velocity imposed at the bottom face of the entire channel length.

These CFD simulations were completed with a software package by Fluent, Inc., similar to that used by Walters and Leylek (1996), Martin and Thole (1997) and Kohli and Thole (1997). An unstructured mesh was used for these studies whereby grid adaptions are based on the gradients of flow variables of the solutions to achieve grid independent results. Second-order discretization was used for the governing equations for momentum, energy, and turbulence. Turbulence closure was achieved by using the standard k-ε model (Launder and Spalding, 1974) with nonequilibrium wall functions (Kim and Choudhury, 1995).

Figure 3 shows the initial grid for the diffused film-cooling hole before adaption. The average cell skewness for the tetrahedral unstructured grids was 0.33 with the cells near the wall maintaining an average height of $y^+ = 20$, which was required in order to use the wall function approach correctly. The average number of cells for the shaped hole simulations was 180,000 for the half-hole simulations and 220,000 cells for the entire hole. Typically, each simulation was split into six partitions and was run in parallel on an IBM SP/2 computer. Solution initialization was done using the freestream velocity and temperature and flow solutions were obtained using an under-relaxation parameter of 0.2 for momentum, k and ε. For each case, a solution to the momentum equation (with the supply channel at the freestream temperature) was obtained before beginning the energy solution (with the supply channel temperature such that DR = 2). To insure that a grid independent solution was obtained, it was verified that further gradient adaption changed the value of laterally averaged effectiveness monitored near the hole by less than $\Delta\eta = 0.005$. The total number of iterations required for convergence was about 2000. For these solutions, values of centerline and laterally averaged effectiveness monitored near the hole over the last 1000 iterations changed by less than $\Delta\eta_{cl} = 0.001$ and $\Delta\bar{\eta} = 0.0001$ respectively. At the same time values of the velocity magnitude monitored over and inside the film cooling hole changed less than $\Delta V = 0.003$ m/s.

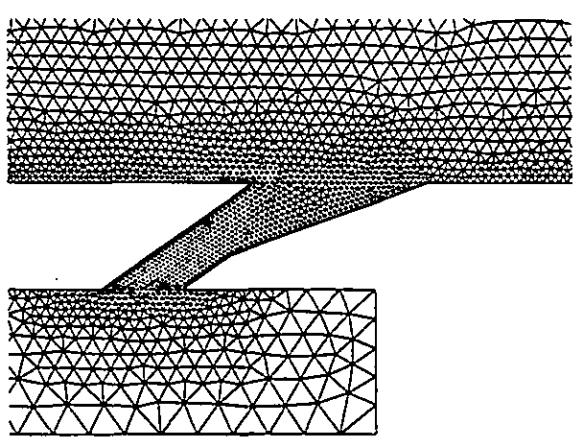

Fig. 3 An example of the intial unstructured grid used for the simulations in this study.

Hole Geometries and Test Cases

The fully diffused cooling hole geometry used for this study was angled at $\alpha = 35°$ to the mainstream, had a hole diameter of D = 12.7 mm, and a length-to-diameter ratio of L/D = 4 as shown in Figure 1. For the baseline case, the length of the cylindrical metering length was $L_M/D = 2$, after which it expanded at 15° in both the forward and lateral directions. In the expanded portion of the cooling hole the inside corners were rounded to have a radius of one-half the hole diameter. At the hole exit plane, the cooling hole had a streamwise extent of 3.8D and a spanwise extent of 1.8D. For all simulations in this study the cooling holes were considered to be spaced P/D = 6 apart, the density ratio was kept fixed at DR = 2, and the mainstream velocity at the hole exit was kept fixed at 10 m/s. Note that the origin for the cooling hole is at the center of the cylindrical part of the hole projected onto the exit plane.

Table 1a shows the two blowing ratios and four different crossflow cases investigated for the coolant supply channel. These four crossflow cases were a plenum supply, a supply channel that was co-flowing ($\phi = 0°$) or counter-flowing ($\phi = 180°$), and a supply channel that was flowing in a direction perpendicular to the mainstream flow ($\phi = 90°$). For the $\phi = 0°, 90°$, and 180° cases, the supply channel velocity and height was set to 3.5 m/s and H/D = 3, which provided a channel Reynolds number of Re = 30,000. This channel Reynolds number and a metering length of $L_M/D = 2$ was used for all the cases listed in Table 1a.

The test matrix for studying the effect of the supply channel Reynolds number is shown in Table 1b. The three different Reynolds numbers were achieved by using supply channel inlet velocities of 1.17, 3.5, and 10.5 m/s. These cases were done for a crossflow angle of $\phi = 90°$ and a metering length of $L_M/D = 2$. Table 1c lists the cases used to study the effect of changing the metering length. Two different crossflow conditions were used to study the effect of changing the metering length between $1 < L_M/D < 4$. In all, fourteen cases were used to study the effects of changing different parameters affecting the film-cooling performance.

Table 1a. Test Matrix for Blowing Ratio and Channel Orientation Effects

	$L_M/D = 2$, Re = 30,000			
	Plenum	$\phi = 0°$	$\phi = 90°$	$\phi = 180°$
M = 1	√	√	√	√
M = 2	√	√	√	√

Table 1b. Test Matrix for Channel Reynolds Number Effects

	$L_M/D = 2$, $\phi = 90°$		
	Re = 10,000	Re = 30,000	Re = 90,000
M = 2	√	√	√

Table 1c. Test Matrix for Metering Length Effects

	Re = 30,000, M = 2		
	$L_M/D = 1$	$L_M/D = 2$	$L_M/D = 4$
Plenum	√	√	√
$\phi = 90°$	√	√	√

Results

The following sections discuss the predictions of the film-cooling performance obtained for the test matrix given in Tables 1a-c. In each section of the results comparison will be made to relevant data available in the open literature. Prior to discussing the adiabatic effectiveness values, the discharge coefficients for each case will be presented. For each parameter being studied, first the laterally averaged surface adiabatic results are presented. Next, the extent of ingestion into the film-cooling hole is discussed. For some cases additional results in terms of surface contours of adiabatic effectiveness and details of the flow inside the film-cooling hole are provided to explain the observed trends.

Discharge Coefficient Results

Comparing discharge coefficients is important because it represents one check on how accurately the flow through the cooling hole is being predicted. This comparison is made difficult because of the fact that these results are for very low pressure ratios ($P_c/p_\infty \sim 1.02$) which typically have higher experimental uncertainties. Most experimental data available in the literature are for much higher pressure ratios and different hole geometries, such as a round hole. Thus, comparisons to the literature were also made using results from our previous paper (Kohli and Thole, 1997) which included a round hole geometry. Table 2a gives the results for the round hole and are compared with data from the literature. Note that our data is for a cooling hole length-to-diameter ratio of L/D = 4 inclined at 35° while the data from the literature is for an L/D = 6 inclined at 30°. Overall there is good agreement between the predicted and measured values.

Table 2a. Discharge Coefficients for a Round Film-Cooling Hole

Cross-Flow	P_c/p_∞	C_D	C_D from Literature
Plenum	1.011	0.51	0.51 from Gritsch, et al. (1997b)
$\phi = 0°$	1.002	0.55	0.50 from Hay, et al. (1983)
$\phi = 90°$	1.004	0.43	

Table 2b gives the discharge coefficients for all of the CFD cases that were investigated for the diffused film cooling hole. Note that all the pressure ratios for the diffused film-cooling hole are quite small at $P_c/p_\infty \sim 1.02$. The one comparison that can be made to the literature is for the case of the plenum with $L_M/D = 4$. Data from Gritsch, et al. (1997b) indicates a $C_D = 0.78$ as compared with our predictions of $C_D = 0.81$.

There are a number of evident trends from these predicted results. As the hole metering length increases, the discharge coefficient increases. Hay and Lampard (1995) showed similar trends for a 90° flared hole at low pressure ratios. There is a clear effect of the crossflow orientation on the discharge coefficient as indicated for the $L_M/D = 2$ cases. For example, at M = 1 the discharge coefficient ranged between $0.55 < C_D < 1.04$ for the different crossflow orientations. Note that a discharge coefficient greater than unity indicates that there may be a slight pressure recovery through the diffuser of the cooling hole as also discussed by Gritsch, et al. (1997).

Another trend which can be seen from the results is that the discharge coefficient decreases with increasing supply channel Reynolds numbers. This is consistent with the results presented by both Rohde, et al. (1969) and Byerley, et al. (1988) who showed that for lower velocity head (higher channel Reynolds numbers), there is a decrease in the discharge coefficient.

Table 2b. Discharge Coefficients for a Diffused Film-Cooling Hole

	Cross-Flow	M = 1	M = 2
$L_M/D = 1$, Re = 30,000	Plenum		0.66
$L_M/D = 1$, Re = 30,000	$\phi = 90°$		0.67
$L_M/D = 2$, Re = 30,000	Plenum	0.77	0.77
$L_M/D = 2$, Re = 30,000	$\phi = 0°$	1.04	0.90
$L_M/D = 2$, Re = 30,000	$\phi = 180°$	0.55	0.64
$L_M/D = 2$, Re = 30,000	$\phi = 90°$	0.68	0.72
$L_M/D = 4$, Re = 30,000	Plenum		0.81
$L_M/D = 4$, Re = 30,000	$\phi = 90°$		0.78
$L_M/D = 2$, Re = 10,000	$\phi = 90°$		0.76
$L_M/D = 2$, Re = 90,000	$\phi = 90°$		0.62

In addition to good agreement between the predicted and measured discharge coefficients, flowfield comparisons were also made to the data presented by Thole, et al. (1997) who measured very high turbulence levels exiting the diffused cooling hole. The exiting turbulence levels from the holes are comparable to those measured, between 10% ≤ Tu ≤ 14% for M = 1. These high turbulence levels were due to the jet being separated inside the cooling hole, as is predicted in all of our simulations of the 15° diffused cooling hole. Both the discharge coefficient agreement and turbulence level predictions give us confidence in our ability to predict the flow through these diffused film-cooling holes.

Results

This section presents the adiabatic effectiveness predictions for the various test cases previously described. The effects of different channel orientations at two mass flux ratios will be discussed followed by discussions on the effect of channel Reynolds number and hole metering length.

Effect of Supply Channel Orientation at Different Mass Flux Ratios

The effects of blowing ratio and supply channel orientation on the laterally averaged adiabatic effectiveness are shown in Figure 4a. Also shown in Figure 4a is a comparison of our predictions with the experimental data of Gritsch, et al. (1997a) where the agreement is very good for the plenum case. As expected, the high blowing ratio case of M = 2 outperforms the M = 1 case for all supply channel orientations with the exception of very close to the cooling hole for the $\phi = 90°$ case. The CFD predictions indicate that similar effects are seen at both blowing ratios with the $\phi = 0°$ case having slightly higher laterally averaged effectiveness values than the plenum case. The $\phi = 180°$ case shows effectiveness values similar to those of the plenum case. For both blowing ratios there is a significant reduction of effectiveness for the $\phi = 90°$ coolant channel crossflow with a larger effect occurring at M = 2. This is consistent with the experimental results presented by Gritsch, et al. (1997a) who showed a larger change in the reduction of effectiveness levels at higher blowing ratios for high freestream Mach numbers of $Ma_\infty = 0.6$. This is not only relevant from a film-cooling design perspective, but is also important when using experimental data from film-cooling studies whereby the cooling hole was supplied by a plenum.

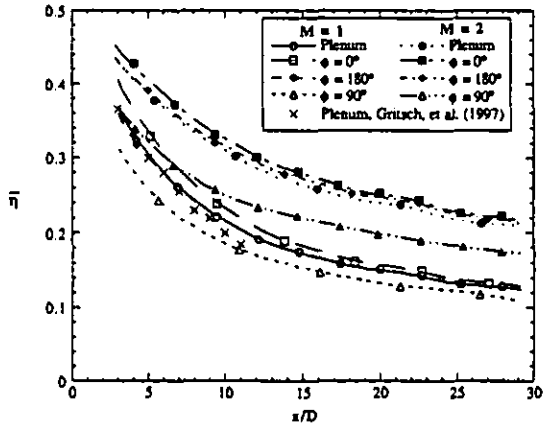

Fig. 4a Laterelly averaged effectiveness as a function of blowing ratio and supply channel orientation for $L_M/D = 2$ and Re = 30,000.

The local adiabatic effectiveness contours for the plenum and $\phi = 90°$ cases at M = 2 are given in Figure 4b. Note that the orientation of the supply channel flow is in the -z direction and that the contours for the plenum case have been mirrored to get a complete view. These contours clearly show a very skewed jet exiting the film-cooling hole for the $\phi = 90°$ case. Although the peak levels extend further downstream for the $\phi = 90°$ case in the near-hole region, the overall width of the jet is much narrower. Although the $\phi = 0°$ and 180° are not shown here, the contours are very similar to the plenum case. These predictions indicate the same effects at M = 1 (Kohli and Thole, 1997).

Figure 4c presents the hot mainstream ingestion within the film-cooling hole. These values are the spatially-averaged jet temperatures at a given depth inside the cooling hole where $\bar{\Theta} = 1$ represents undiluted jet fluid. Note that y is measured vertically down into the hole from the top plate surface and y/D = -1.55 is at the start of the hole expansion. As can be seen in Figure 4b, ingestion inside the film-cooling hole is significantly larger for the $\phi = 90°$ case for both blowing ratios in comparison with the other supply channel orientations. The co-flowing channel is slightly better than the other orientations. Note that the larger reduction in effectiveness for the higher blowing ratio case of M = 2 also corresponds to the case having the deepest ingestion into the film-cooling hole.

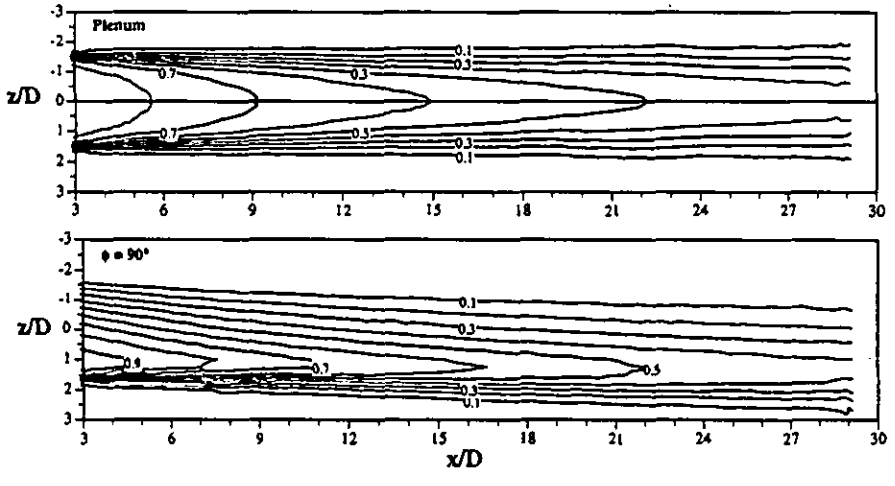

Fig. 4b Effect of supply channel orientation on the surface adiabatic effectiveness for M = 2, $L_M/D = 2$, and Re = 30,000.

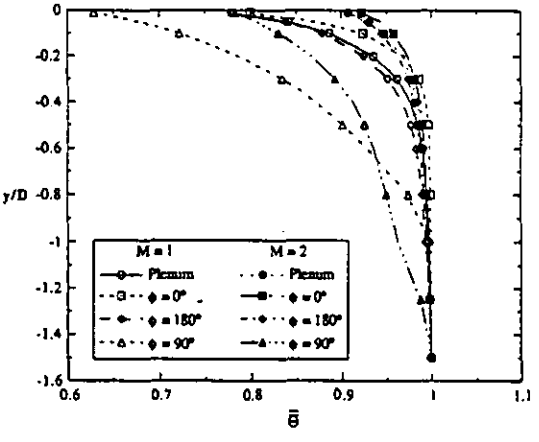

Fig. 4c Ingestion within the film-cooling hole as a function of blowing ratio and supply channel orientation for $L_M/D = 2$ and Re = 30,000.

Effect of Channel Reynolds Number

The effect of channel Reynolds number was investigated for a metering length-to-diameter ratio of $L_M/D = 2$ and supply channel orientation of $\phi = 90^\circ$. Figure 5a shows the laterally averaged effectiveness values for supply channel Reynolds numbers between $10{,}000 < Re < 90{,}000$. These supply channel Reynolds numbers are typical of those found in internal cooling passages of turbine blades (Han, 1984). Except in the near-hole region, the results for Re = 30,000 and 90,000 are very similar. There is a significant improvement in effectiveness, however, for the lowest Reynolds number investigated in this study, Re = 10,000.

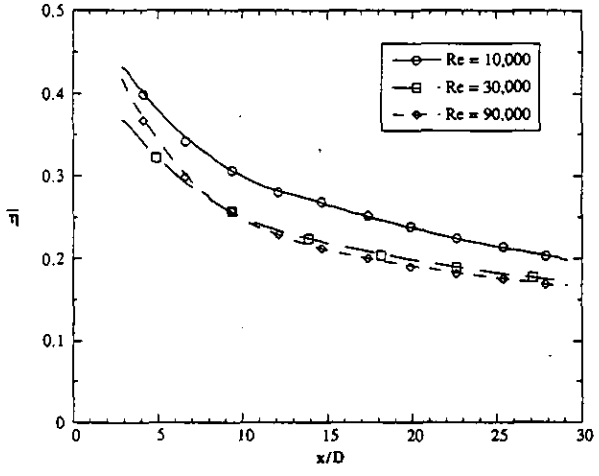

Fig. 5a Laterally averaged effectiveness as a function of supply channel Reynolds number for M = 2, $\phi = 90^\circ$, and $L_M/D = 2$.

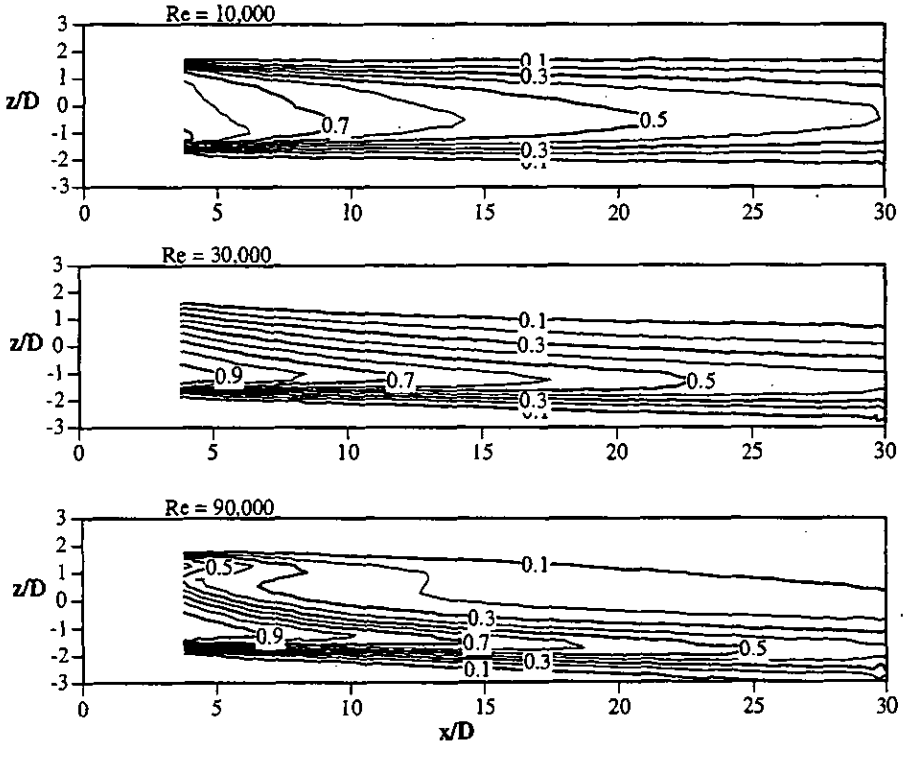

Fig. 5b Effect of supply channel Reynolds number on the surface adiabatic effectiveness for M = 2, $\phi = 90^\circ$, and $L_M/D = 2$.

Unlike the laterally averaged effectiveness results, a drastic difference is seen in the surface adiabatic contour patterns between the Re = 30,000 and 90,000 cases. Figure 5b shows that for both the Re = 10,000 and 30,000 cases the jet exits in a skewed manner. As the Reynolds is increased to Re = 90,000 in addition to the peak seen for the lower Reynolds number cases, a second lower peak in effectiveness occurs on the -z side of the hole. This second peak causes the increased average effectiveness values in the near-hole region as was shown in Figure 5a.

These double peaks in the surface effectiveness were also reported by Gritsch et al. (1997a) for their M = 1 case with a strong $\phi = 90^\circ$ crossflow. The difference, however, between these predictions and the measurements of Gritsch, et al. (1997a) is that the larger peak occurs on opposite sides of the cooling hole with respect to the direction of the crossflow at the hole entrance. These predictions indicate that the larger peak is on the channel flow upstream side of the hole while their measurements indicate it is on the downstream side of the hole. This can be explained by the fact that their cooling hole has an L/D = 6 which allows the jet to complete another half-turn before exiting the hole, as shown in Figure 5c by the pathlines inside the hole.

Figure 5c shows the pathlines inside the film-cooling hole for the high and low Reynolds number cases respectively. As seen in Figure 5c, for the high Reynolds number case, the pathlines indicate a strong turning of the jet as it progresses through the hole with the higher jet velocities exiting from the +z direction of the hole. At the low Reynolds number, however, there is hardly any turning inside the hole.

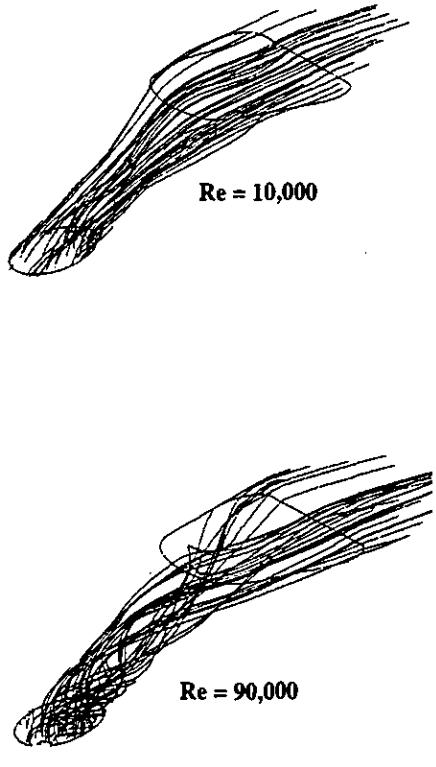

Fig. 5c Pathlines inside the film-cooling hole for two supply channel Reynolds numbers for M = 2, $\phi = 90^\circ$, and $L_M/D = 2$.

Effect of Hole Metering Length

Three different metering lengths were simulated for a blowing ratio of M = 2 with a Reynolds number of Re = 30,000. The laterally averaged effectiveness results for the plenum and $\phi = 90^\circ$ cases are shown in Figure 6a. Results for the plenum case show that there is a small effect with the smallest metering length having a lower averaged effectiveness in the near-hole region compared to the longer metering length holes. This disadvantage, however, in the near-hole region is counter-balanced with the higher average effectiveness values beyond x/D = 10. This near-hole effect can be explained by the fact that at the shortest metering length the exiting jet has a higher trajectory causing a lower effectiveness. For the same reason, further downstream there is a higher effectiveness compared to the longer metering lengths.

For the $\phi = 90^\circ$ case, there is a significant reduction in the lateral averaged effectiveness for the longer metering length hole. It is quite surprising that as the metering length of the hole becomes longer, there is a continued reduction in effectiveness. These results can be explained by examining the flow inside the cooling hole. Figure 6b shows the velocity vectors on a vertical plane at the hole centerline, which is not a plane of symmetry for this $\phi = 90^\circ$ case. For the longer metering length, there is a small separation bubble at the hole entrance, but there is enough hole length for the jet to reattach. There is only a slight separation near the exit of the hole. In contrast for a small metering length the jet is unable to reattach before the expansion occurs thereby causing a very strong jetting action which pushes the jet towards the windward side of the hole. This jetting action deflects the mainstream and actually reduces the amount of hot mainstream ingestion inside the hole, as shown in Figure 6c. For this reason we see an improved performance in terms of adiabatic effectiveness. A larger separation region for a smaller metering length is expected based on the discharge coefficients discussed earlier whereby lower C_D values occurred at smaller L_M/D.

These results are key in operating with a 15° diffused cooling hole used in combination with a 90° coolant supply channel orientation. These results indicate that it is, in fact, beneficial to have separation inside a diffused cooling hole. This is further illustrated for the plenum case in which the flow is completely separated for all the metering length cases and shows unchanged and relatively good performance in laterally averaged effectiveness values. Improved effectiveness values occur because a large portion of the jet exiting the hole is protected by the upstream hole jetting effect. In addition because the jet is exiting from the upstream portion of the hole, there is enough streamwise distance to allow the jet to be pushed down before encountering the downstream surface.

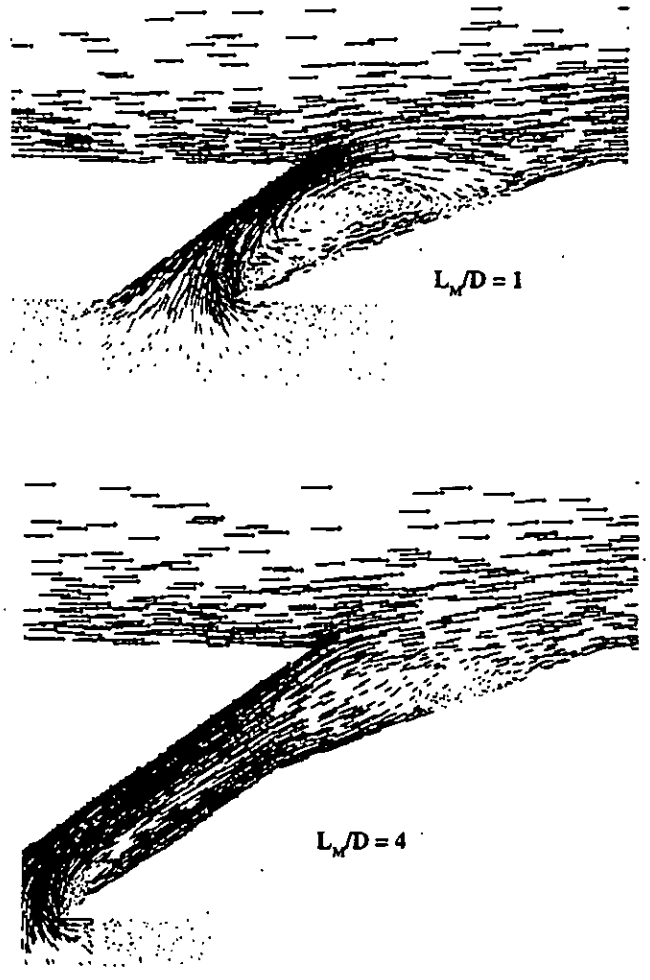

Fig. 6b Velocity vectors on a vertical plane at the jet centerline for two metering lengths for $\phi = 90^\circ$, M = 2 and Re = 30,000.

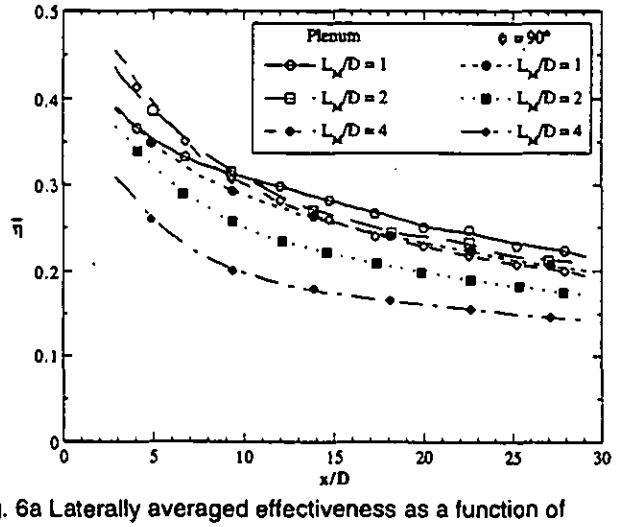

Fig. 6a Laterally averaged effectiveness as a function of metering length for M = 2 and Re = 30,000.

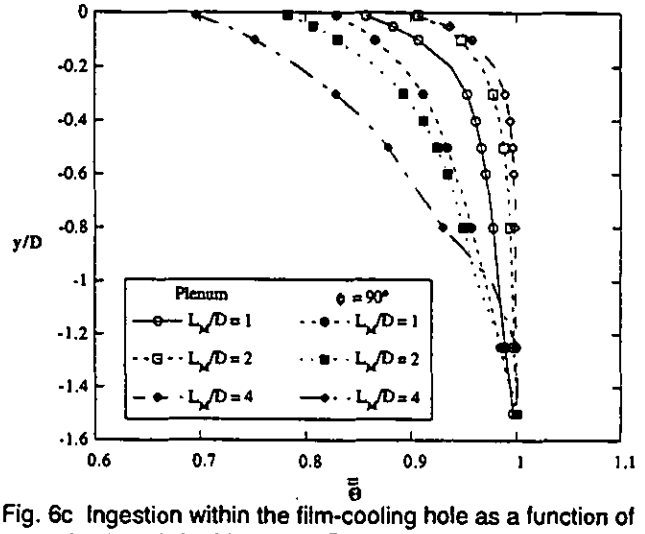

Fig. 6c Ingestion within the film-cooling hole as a function of metering length for M = 2 and Re = 30,000.

Conclusions

This study, which agreed with the trends of the experimental data available in the open literature, has presented a number of different possible geometry and flow parameter variations for a 15° diffused cooling hole. For obvious reasons, such as a wider coverage and sustained effectiveness over a range of blowing ratios, diffused cooling holes are desirable. These results indicate how best to use a diffused cooling hole for different regions on a turbine blade where the internal cooling configuration could have different supply channel orienations and Reynolds numbers.

The effect of the channel Reynolds number is such that it can completely change the footprint of the adiabatic effectiveness contours. With a higher channel Reynolds number for a perpendicular crossflow, the cooling jet was split as it exited the hole. This split was attributed to the fact that there was a sustained, stronger jet turning inside the cooling hole.

The coolant channel crossflow orientation was shown to play a major role on the discharge coefficients and effectiveness values for different blowing ratios. The counter-flowing and co-flowing results were very similar to that of a stagnant plenum. In general, the supply channel crossflow has the largest detrimental effect when it is perpendicular to the mainstream direction. However, this effect can be nullified by using a short metering length such that the flow is completely separated with a strong jetting action on the upstream side of the hole to deflect the mainstream.

Acknowledgements

The authors would like to thank the National Science Foundation for supporting this work through the CAREER Award.

References

Berhe, M. K. and Patankar, V. (1996) "A Numerical Study of Discrete-Hole Film Cooling," ASME Paper No. 96-WA/HT-8.

Burd, S. W. and Simon, T. W. (1997) "The Influence of Coolant Supply Geometry on Film Coolant Exit Flow and Surface Adiabatic Effectiveness," ASME Paper No. 97-GT-25.

Byerley, A. R., Ireland, P. T., Jones, T. V., and Ashton, S.A. (1988) "Detailed Heat Transfer Measurements Near and Within the Entrance of a Film-Cooling Hole," ASME Paper No. 88-GT-155.

FLUENT User's Guide (1996) Fluent Incorporated, Lebanon, New Hampshire.

Gritsch, M., Schulz, A., and Wittig, S. (1997a) "Adiabatic Wall Effectiveness Measurements of Film-Cooling Holes with Expanded Exits," ASME Paper No. 97-GT-164.

Gritsch, M., Schulz, A., and Wittig, S. (1997b) "Discharge Coefficient Measurements of Film-Cooling Holes with Expanded Exits," ASME Paper No. 97-GT-165.

Han, J. C. (1984) "Heat Transfer and Friction in Channels with Two Opposite Rib-Roughened Walls," ASME Journal of Heat Transfer, Vol. 106, pp. 774-781.

Hay, N., Lampard, D., and Benmansour, S. (1983) "Effect of Crossflows on the Discharge Coefficient of Film Cooling Holes," ASME Journal of Engineering for Power, Vol. 105, pp. 243-248.

Kim, S. and Choudhury, D. (1995) "A Near-Wall Treatment Using Wall Functions Sensitized to Pressure Gradient," ASME Fluids Engineering Div. Summer Conference, Hilton Head, South Carolina.

Kohli, A. and Thole, K. A. (1997) "A CFD Investigation on the Effect of Entrance Flow Conditions in Discrete Film Cooling Holes," ASME Proceedings of the 32nd National Heat Transfer Conference Vol. 12, pp 223-232.

Launder, B. E. and Spalding, D. B. (1974) "The Numerical Computation of Turbulent Flows," Computer Methods in Applied Mechanics and Engineering, Vol. 3, pp. 269-289.

Martin, C. and Thole, K. A. (1997) "A CFD Benchmark Study: Leading Edge Film Cooling with Compound Angle Injection," ASME Paper No.97-GT-297 .

Rohde, J. E., Richards, H. T., Metger, G. W. (1969) "Discharge Coefficients for Thick Plate Orifices with Approach Flow Perpendicular and Inclined to the Orifice Axis," NASA TN D-5467.

Sinha, A. K., Bogard, D. G., Crawford, M. E. (1991) "Film Cooling Effectiveness Downstream of a Single Row of Holes with Variable Density Ratio," ASME Journal of Turbomachinery, Vol. 113, pp. 442-449.

Thole, K. A., Gritsch, M., Schulz, A., and Wittig, S. (1996) "Flowfield Measurements for Film Cooling Holes with Expanded Exits," ASME Paper No. 96-GT-174, to appear in the ASME Journal of Turbomachinery.

Thole, K. A., Gritsch, M., Schulz, A., and Wittig, S. (1997) "Effect of a Crossflow at the Entrance to a Film-Cooling Hole," ASME Journal of Fluids Engineering, vol. 119, pp. 533-540.

Walters, D. K. and Leylek, J. H. (1996) "A Systematic Computational Methodology Applied to a Three-Dimensional Film-Cooling Flowfield," ASME Paper No. 96-GT-351.